An IT-Guided Design of Smart Bio-Nanocomposite Films for Next-Generation Antimicrobial Wound

Salih Nasser Rahmah and Mahdi A. Mohammed
Department of Physics, College of Science, Wasit University, 52001 Al-Kut, Wasit, Iraq
std2023204.ssuhain@uowasit.edu.iq

Keywords: Electrospinning, Nanofibers, PVA, GA, GO.

Abstract: In recent years, electrospinning has gained significant attention for the production of innovative nanofibrous materials with diverse applications in science and engineering. The use of graphene oxide and natural products derived from plants and/or trees has gained remarkable popularity in many scientific disciplines due to their availability, eco-friendliness, and unique properties. In this study, an approach is presented for producing nanofibers using a carefully prepared mixture of 2 wt% Gum Arabic (GA), a natural tree gum extract, 8 wt% Polyvinyl alcohol (PVA), an environmentally friendly stabilizer, and 0.5 wt% Graphene Oxide (GO), which was incorporated to enhance the durability and performance of the fabricated nanofibers. The electrospinning process was carried out using a laboratory-made electrospinning system under controlled conditions. X-ray diffraction (XRD) and field emission scanning electron microscope (FESEM) analysis were employed to characterize the GO. Furthermore, FESEM was also utilized to investigate the morphology, distribution, and diameters of the nanocomposite fibers.

1 INTRODUCTION

In recent years, electrospinning has become a widely recognized method for fabricating polymer nanofibers with adjustable diameters and morphologies through the regulation of processing and solution variables. Consequently, electrospinning has been extensively employed as an effective technique for fabricating composite nanofibers [1]. Moreover, the design versatility and component controllability of electrospun nanofibers are considerable advantages. Due to the superior characteristics derived from these structural benefits, electrospun nanofibers possess significant potential for extensive application in protective textiles, filtration, composite reinforcement, and biomedical fields, including tissue engineering scaffolds, wound dressings, and drug delivery systems [2].

Nanomaterials have demonstrated excellent properties that surpass those of bulk materials in various fields [3] - [6]. One of the most interesting materials is graphene oxide (GO). It has recently been regarded as an essential material in the domain of carbon nanostructures. GO resembles graphene, with the hexagonal planes of graphene adorned by oxygen atoms. The presence of oxygen-containing functional groups (hydroxyl, epoxy, and carboxyl) on the GO surface makes it more hydrophilic and easier to spread in water and other polar solvents. The remarkable chemical and physical features of GO render it highly effective in catalysis [7], [8], energy [9], and drug delivery [10], as well as numerous further applications [11] - [15].

The polydispersity of the graphene/polymer solution before the electrospinning process is a critical component in the manufacturing of graphene-based nanofibers. Numerous materials have been evaluated as co-blending solutions for nanofiber manufacturing [16]; Nonetheless, there exists a significant deficiency in the utilization of "green" polymers (for instance, tree-derived gums [17], [18]) for this purpose. This can render the entire process more sustainable and cost-effective. Consequently, we have endeavored to close this gap by utilizing GA as a renewable, eco-friendly, biodegradable agent for the synthesis of graphene-based nanofibers. GA or Acacia gum is the exudate from the Acacia Senegal and Acacia seyal trees, which are part of the Leguminosae family. It is a complex, branching heteropolysaccharide, either neutral or somewhat acidic, and composed of 1, 3-linked β-D-galactopyranosyl units. L-arabinose, L-rhamnose, and D-glucuronic Acids have also been identified as

components of this polymer [19]. The side chains consist of two to five 1, 3-linked β-D-galactopyranosyl units that connect to the primary chain through 1, 6-linkages [20]. Historically, PVA has proven to be a superior co-solvent in gum solutions for the electrospinning process, markedly outperforming PEO (polyethylene oxide) [21]. Despite substantial research on electrospun polymer and polymer/graphene-based nanofibers, controlling fiber continuity and morphology while preserving environmental sustainability is still a challenge. Many biopolymers show poor mechanical stability or restricted spinning ability, which limits their practical application.

In the present study, a ternary PVA/GA/GO composite system is constructed in which each component serves a specific function. The PVA is selected as the main matrix due to its superior electrospinning ability, mechanical stability, and water solubility [22]. The GA, a naturally occurring and biodegradable polysaccharide, is used as a green modifier to improve intermolecular interactions and solution viscosity; nevertheless, when used alone, its high molecular complexity may have a negative impact on jet stability. It must add to synathic polymer to produce fibers [23]. Incorporating the GO as an electrically conductive and nanoscale reinforcing filler enhances the mechanical properties of fibers and modifies optical properties [24]. The purpose of this work is to understand how fiber production and optical behavior in electrospun nanofibers are influenced by the synergistic combination of PVA, GA, and GO.

2 EXPERIMENTAL PART

2.1 Materials

All chemicals used in this study were of analytical grade. Polyvinyl alcohol molecular formula (C4H6O2C2H4O)X, 67000 g/mol molecular weight, 1400 degree of polymerization, 88% degree of hydrolysis, viscosity of 8 mPa.s (in 4% aqueous solution), and physical form pure, solid, white, odorless, granular. It was purchased from ME Scientific Engineering Ltd. GA was purchased from THOMAS BAKER, India, with maximum impurity limits: acid-insoluble ash of 1.0%, water-insoluble matter of 1.0%, loss of 15.0% on drying at 105 °C, and 5.0% sulfated ash. GO was purchased from Platonic Nano Private Limited, India, with a purity of 98%, APS (Average Particle Size) of 20 nm, and a thickness of less than 5 nm.

2.2. Preparation of PVA/GA/GO Solutions

In the first step, a PVA solution was prepared by adding 1 gram of PVA polymer to 10 ml of deionized water and homogenizing the solution at 80 °C with continuous stirring for 60 minutes.

In the second stage, a PVA-GA solution was prepared by adding 0.8 grams of the synthetic polymer PVA in 10 ml of deionized water and mixing them as in the first step under continuous stirring at a temperature of 80 °C for 60 minutes. Then, 0.2 grams of GA was added to the solution and left to homogenize overnight under continuous stirring.

In the final stage of preparation, a GO solution was prepared by dissolving 0.05 grams of graphene oxide in 10 ml of deionized water. This mixture was ultrasonicated for 70 minutes to achieve a fine and even consistency. After the dispersion process was completed, the solution was transferred to a magnetic mixing device, where 0.8 grams of PVA were added to the mixture. The mixing process continued for 90 minutes at 80 °C to ensure complete dissolution and homogeneity of the polymer. Then, 0.2 grams of GA were added to the mixture, with continuous magnetic stirring overnight to ensure optimal homogeneity and achieve the desired physical and chemical properties of the resulting solution.

2.3 Electrospinning Process

A laboratory-scale electrospinning system was used to produce nanofibers. This system includes a high-voltage power supply (HVPS) capable of delivering up to 30,000 V with integrated voltage measurement, an acrylic injection pump with Bluetooth connectivity for wireless control and Arduino-based modification, and an aluminum sheet accumulator to ensure electrical conductivity. Two electronic circuits manage the HVPS and injection pump, providing operational precision and adaptability.

Prepared solutions were loaded into a 5 ml syringe within our lab-built electrospinning system. This system comprises a smart syringe pump, a high-voltage power supply, and a collector. Electrospinning was performed with a 16 cm needle-collector distance, a 30 kV voltage, and a 0.02 ml/min flow rate.

2.4 Characterization

XRD (Shimadzu-6000, Japan; 1.2 kW; Cu) with a wavelength of 1.5406 Å was used for the characterization of GO.

The morphology of the prepared nanofibers was observed using a FESEM (Nova NanoSEM 450, FEI, USA, and Axia ChemiSEM, Thermo Fisher Scientific, USA, and TESCAN Vega2, Czech Republic). Before analysis, the samples were sputter-coated with gold to improve conductivity during imaging. To determine the average diameters and diameter distribution of the prepared nanofibers, 40 different fibers were randomly selected, and their diameters were measured using ImageJ software.

A UV-visible spectrometer (DU-8800, DRAWELL, China) was used to study the optical properties of the prepared samples.

3 RESULTS AND DISCUSSION

3.1 XRD and FESEM Analysis of GO

GO was analyzed via XRD and FESEM, as depicted in Figure 1. The XRD pattern reveals significant peaks, notably at 10°, associated with the (001) plane, reflecting interlayer spacing attributed to oxygen functionalities [25]. Conversely, the weak peak at 42° pertains to a short-range order inside the layers of stacked graphene, which are characteristic of the semicrystalline profile of the turbostratic graphite structure [26] - [29]. The FESEM image of GO reveals a broad surface and an intricate sheet with a smooth morphology. The GO appears to be thin, transparent, crumpled layers with notable overlapping regions and folded edges. The visible wrinkles and ripples could indicate that the sheets of graphene oxide have a few layers. The edges of the GO sheets are clear and display the thin nature of the material.

3.2 UV-Visible Spectrum

The optical properties of the prepared solutions of PVA, PVA/GA, and PVA/GA/GO were studied using a UV-visible spectrometer. The spectrum exhibits a distinct absorption within the 200-300 nm band, as shown in Figure 2a. No significant absorption occurs above 300 nm, signifying an absence of robust optical response in the visible band. This verifies that PVA alone does not substantially enhance absorption at elevated wavelengths; this demonstrates that PVA alone has limited optical absorption in the visible region. It was seen that pronounced absorption peaks in the range of 200-300 nm, akin to the PVA spectra, albeit with alterations attributable to the influence of GA, see Figure 2b. Nevertheless, there is no notable alteration beyond 300 nm, suggesting that the incorporation of GA did not substantially enhance the optical responsiveness of the solution.

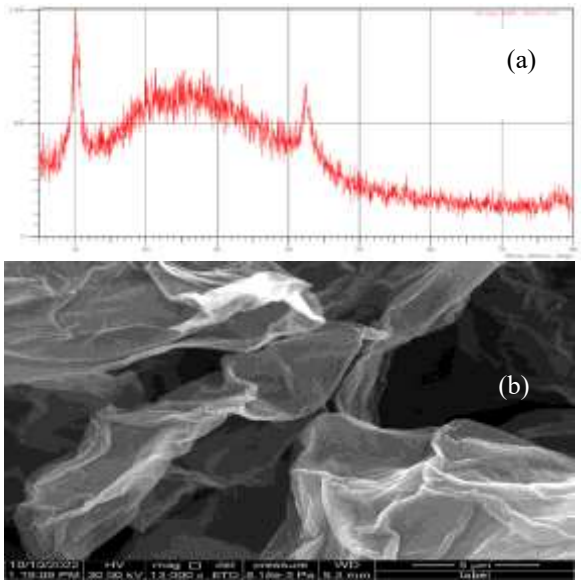

Figure 1: GO characterization: a) XRD analysis of GO and b) FESEM.

Although GA does not considerably widen the absorption range, it may alter other material properties that were not examined in this study. The incorporation of GO results in a notable alteration in the spectrum, as shown in Figure 2c. A notable rise in absorption is observed beyond 250 nm, succeeded by the appearance of a wide absorption band that extends to 400 nm and beyond. This illustrates the characteristics of optical transitions in GO, noted for its significant absorption in ultraviolet and visible light. In contrast to the two preceding solutions, it is evident that GO is the principal element influencing this novel optical response; thus, GO plays a dominating role in changing the optical absorption behavior of the composite.

The energy gaps of the three produced solutions, yielding a value of 5.22 eV for the PVA solution, Figure 3a, which is consistent with [30], 4.95 eV for the PVA-GA solution, Figure 3b, and 4.41 eV for the PVA/GA/GO solution, as shown in Figure 3c. It is clear that the bandgap decreases with the addition of GA and GO in the PVA. The GO is a non-stoichiometric, filled with defects carbon material whose electrical configuration is determined by the arrangement of sp^2 and sp^3 domains rather than a distinct crystalline band structure. The observed reduction in optical band gap following GO integration does not signify typical semiconductor behavior; instead, it demonstrates improved

electronic coupling, defect-state absorption, and π–π* interactions between GO sheets and the polymer matrix. Comparable decreases in the apparent optical band gap following the insertion of graphene oxide into polymer matrices have been reported, attributable to defect-induced localized states and enhanced charge delocalization [31], [32].

An optical absorption study alone is inadequate to confirm direct applicability in optoelectronic devices; additional electrical and device-level research is necessary.

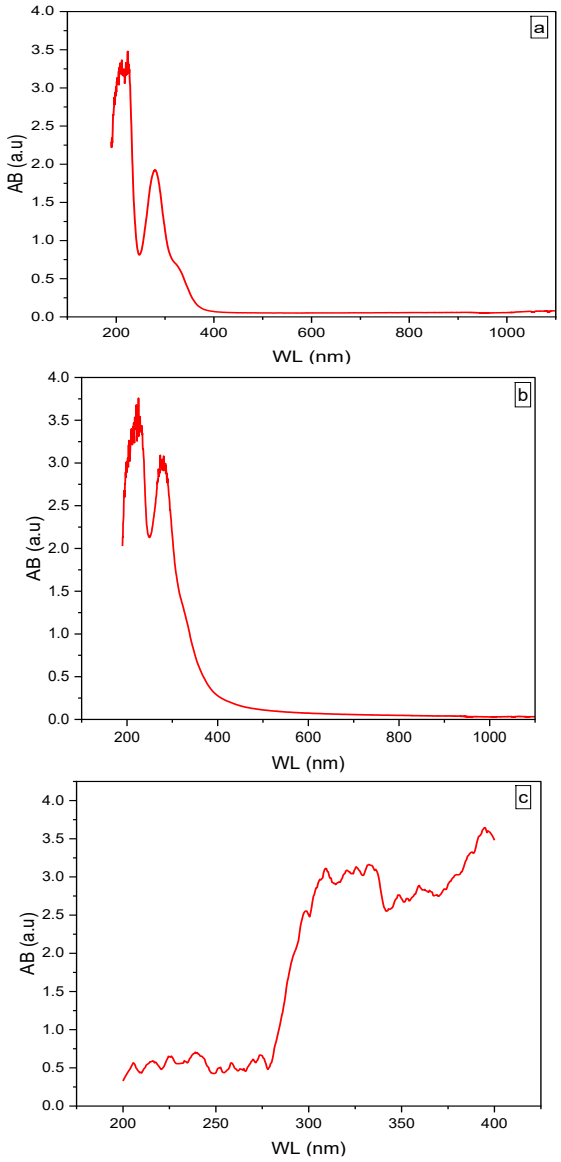

Figure 2: UV-visible spectrum of a) PVA, b) PVA/GA, and c) PVA/GA/GO solutions.

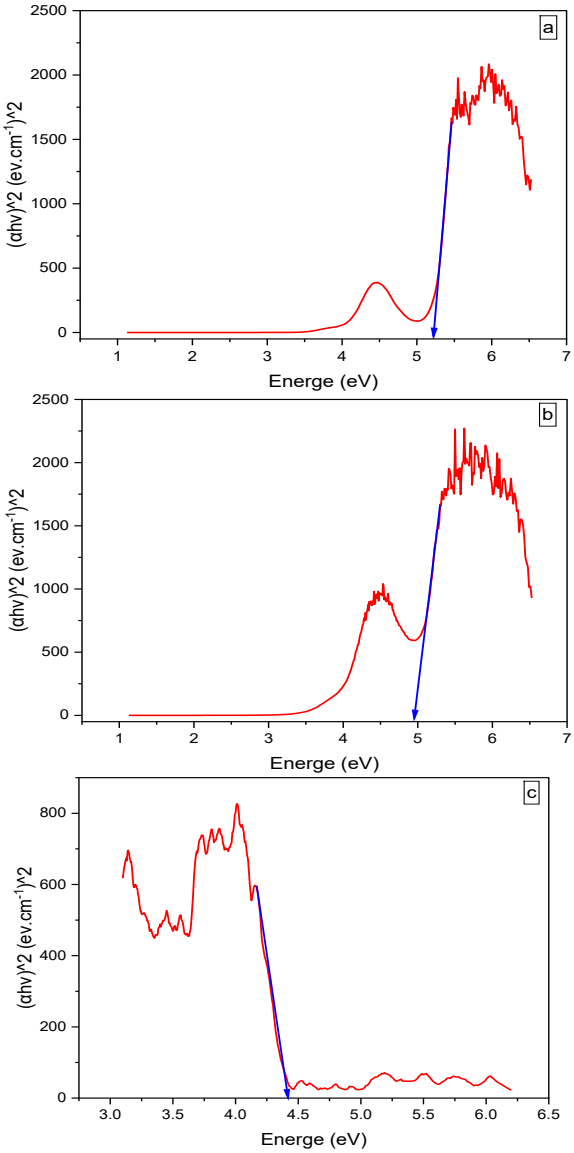

Figure 3: Energy gap of a) PVA, b) PVA/GA, and c) PVA/GA/GO solutions.

3.3 Measurements of Nanofiber Diameters

Although solution viscosity, surface tension, and electrical conductivity were not directly measured in this study, these parameters are well known to have a significant impact on electrospinning behavior. Previous studies have shown that increasing the solution viscosity of the polymer leads to larger fiber diameters [33], [34]. Also, GO is known to reduce fiber diameter by increasing charge density in the jet [35]. Based on recognized electrospinning principles and previously documented patterns in

polymer–polysaccharide and polymer–graphene oxide systems, the observed differences in fiber diameter are therefore qualitatively addressed.

The effect of adding both GA and GO on the formation of PVA nanofibers was studied using a FESEM at 50kx magnification for PVA and PVA/GA and 20kx for PVA/GA/GO. Images were analyzed using ImageJ software to calculate the average diameter of the formed nanofibers, where 50 fibers were measured to determine the diameters. The results showed that the fibers formed from pure PVA were homogeneous and stable, extending to an unlimited length proportional to the amount of solution used, as clearly shown in Figure 4. This result indicates that the base solution is capable of producing continuous, homogeneous fibers under the selected electrospinning conditions.

When 2 wt% GA was added to the solution, 8 wt% of PVA, a significant change in the structure of the resulting fibers was observed, with the fibers appearing discontinuous and irregular, as shown in Figure 5. This change indicates the difficulty of forming cohesive fibers in the presence of GA, which may be due to its effect on the viscosity of the solution or the intermolecular forces during the forming process. GA may have disrupted the flow of the solution during the spinning process, resulting in discontinuous fibers with irregular shape and length.

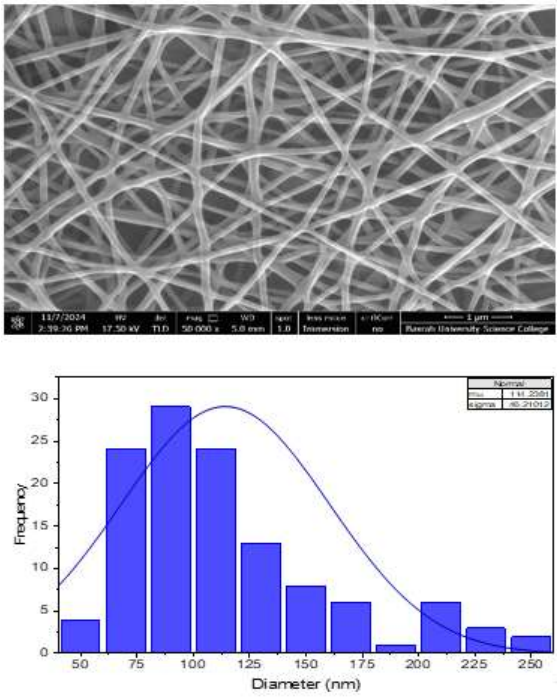

Figure 4: FESEM image of PVA nanofibers and fiber diameter distribution graph using 10 wt% concentration.

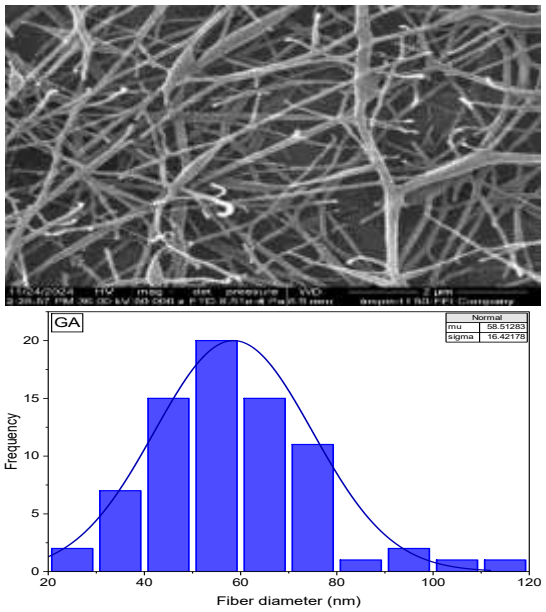

Figure 5: FESEM image of PVA/GA nanofibers and fiber diameter distribution diagram using 2 wt% GA and 8 wt% PVA concentrations.

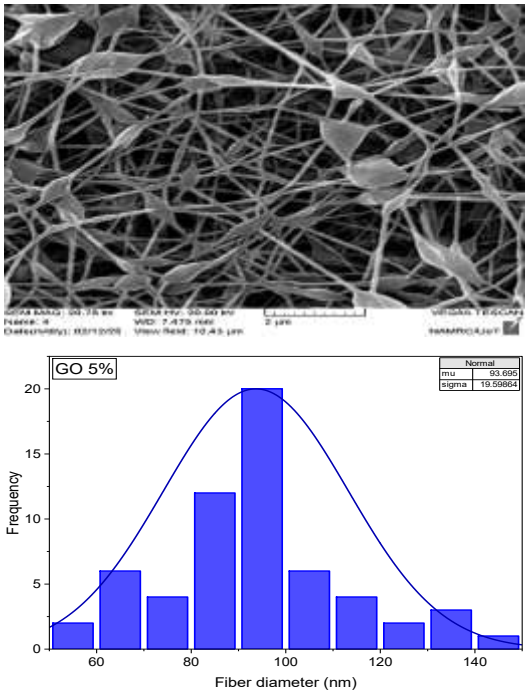

Figure 6: FESEM image of PVA/GA/GO nanofibers and fiber diameter distribution diagram using 2 wt% GA, 8 wt% PVA, and 0.5 wt% GO concentrations.

In an attempt to improve the fiber structure and restore its cohesion, 0.5 wt% GO was mixed with a

solution containing PVA 8 wt% and GA 2 wt%. The results showed that the resulting fibers became more interconnected and continuous, indicating that GO contributed to improving fiber continuity and structural integrity, as shown in Figure 6. This positive effect is attributed to the unique physical and chemical properties of graphene oxide, which likely enhanced the interaction between the various components of the solution, resulting in a more stable and interconnected fiber network.

The creation of continuous electrospun fibers is determined by the balance of solution rheological characteristics and electrical forces acting on the charged jet. The addition of GA, a highly branched polysaccharide, can disrupt polymer chain entanglement and modify solution viscoelasticity, resulting in jet instability and fiber discontinuity. In contrast, adding GO creates conductive channels and raises charge density within the electrospinning jet [35]. This improved electrical conductivity enhances the stretching forces beneath the applied electric field, stabilizing the jet. In addition, GO nanosheets may operate as physical bridges between polymer chains, partially compensating for GA's destabilizing effect and restoring fiber continuity. The seen morphological change can thus be attributed to a combination of GA-induced rheological modification and GO-induced electrical and reinforcing effects.

The mean fiber diameter achieved using pure PVA was found to be 114.23 nm. The incorporation of GA into PVA resulted in a reduction of the average diameters to 58.51 nm. The incorporation of GO into the GA and PVA combination resulted in an increase in average diameters to 93.69 nm.

4 CONCLUSIONS

PVA alone demonstrates minimal absorption in the visible spectrum, with its absorption confined to the ultraviolet range. The incorporation of GA into PVA resulted in a minor alteration of the absorption spectrum, as indicated by the decrease in the energy gap. Adding GO to the mixture significantly improved the absorbance in the visible spectrum, making it the material responsible for the optical modification. The change in optical absorption induced by GO incorporation indicates that the presence of GO would affect the electronic structure of the polymer, which may be of interest for optically sensitive polymer composites.

FESEM results reveal that the incorporation of GA influences fiber continuity and diminishes their diameter, whereas GO enhances the fiber structure's cohesiveness and integrity, increasing the diameter in comparison to GA. This illustrates the possibility of regulating fiber structure and altering its characteristics to suit the needs of specific applications, particularly in applications where controlled fiber morphology is required. Viscosity, surface tension, and electrical conductivity were not measured in this study but will be examined in future studies. Moreover, chemical structure, thermal stability, and mechanical properties need to be considered in future work.

REFERENCES

[1] E. Ghafari, X. Jiang, and N. Lu, “Surface morphology and beta-phase formation of single polyvinylidene fluoride (PVDF) composite nanofibers,” Adv. Compos. Hybrid Mater., vol. 1, no. 2, pp. 332-340, Jun. 2018, [Online]. Available: https://doi.org/10.1007/s42114-017-0016-z.

[2] H. Maleki, A. A. Gharehaghaji, and P. J. Dijkstra, “Electrospinning of continuous poly (L-lactide) yarns: Effect of twist on the morphology, thermal properties and mechanical behavior,” J. Mech. Behav. Biomed. Mater., vol. 71, pp. 231-237, Jul. 2017, [Online]. Available: https://doi.org/10.1016/j.jmbbm.2017.03.031.

[3] N. Baig, I. Kammakakam, and W. Falath, “Nanomaterials: A review of synthesis methods, properties, recent progress, and challenges,” Mater. Adv., vol. 2, pp. 1821-1871, 2021, [Online]. Available: https://doi.org/10.1039/D0MA00807A.

[4] A. Musa, A. Bello, S. M. Adams, et al., “Nano-enhanced polymer composite materials: A review of current advancements and challenges,” Polymers (Basel), vol. 17, p. 893, 2025, [Online]. Available: https://doi.org/10.3390/polym17070893.

[5] M. Pozzi, S. Jonak Dutta, M. Kuntze, et al., “Visualization of the high surface-to-volume ratio of nanomaterials and its consequences,” J. Chem. Educ., vol. 101, pp. 3146-3155, 2024, [Online]. Available: https://doi.org/10.1021/acs.jchemed.4c00089.

[6] Othmani, “Overview of the major types of nanomaterials used for environmental and energy applications: Challenges and prospects,” in D. Tripathi, R. K. Sharma, H. F. Oztop, and R. Natarajan, eds., Springer Nature Singapore, Singapore, pp. 1-13, 2023.

[7] L.-L. Lin, M.-C. Chi, Y.-J. Lan, M.-G. Lin, T.-Y. Juang, and T.-F. Wang, “Facile immobilization of Bacillus licheniformis γ-glutamyltranspeptidase onto graphene oxide nanosheets and its application to the biocatalytic synthesis of γ-l-glutamyl peptides,” Int. J. Biol. Macromol., vol. 117, pp. 1326-1333, Oct. 2018, [Online]. Available: https://doi.org/10.1016/j.ijbiomac.2017.11.153.

[8] B. Majumdar, D. Sarma, T. Bhattacharya, and T. K. Sarma, "Graphene oxide as metal-free catalyst in oxidative dehydrogenative C–N coupling leading to α-ketoamides: Importance of dual catalytic activity," ACS Sustain. Chem. Eng., vol. 5, no. 10, pp. 9286-9294, Oct. 2017, [Online]. Available: https://doi.org/10.1021/acssuschemeng.7b02267.

[9] F. Li, X. Jiang, J. Zhao, and S. Zhang, "Graphene oxide: A promising nanomaterial for energy and environmental applications," Nano Energy, vol. 16, pp. 488-515, Sep. 2015, [Online]. Available: https://doi.org/10.1016/j.nanoen.2015.07.014.

[10] J. Liu, L. Cui, and D. Losic, "Graphene and graphene oxide as new nanocarriers for drug delivery applications," Acta Biomater., vol. 9, no. 12, pp. 9243-9257, Dec. 2013, [Online]. Available: https://doi.org/10.1016/j.actbio.2013.08.016.

[11] S. C. Ray, "Application and uses of graphene oxide and reduced graphene oxide," in Applications of Graphene and Graphene-Oxide Based Nanomaterials, Elsevier, pp. 39-55, 2015, [Online]. Available: https://doi.org/10.1016/B978-0-323-37521-4.00002-9.

[12] X. Xu et al., "Study on the interaction of graphene oxide silver nanocomposites with bovine serum albumin and the formation of nanoparticle-protein corona," Int. J. Biol. Macromol., vol. 116, pp. 492-501, Sep. 2018, [Online]. Available: https://doi.org/10.1016/j.ijbiomac.2018.05.043.

[13] H. Hosseinzadeh and S. Ramin, "Effective removal of copper from aqueous solutions by modified magnetic chitosan/graphene oxide nanocomposites," Int. J. Biol. Macromol., vol. 113, pp. 859-868, Jul. 2018, [Online]. Available: https://doi.org/10.1016/j.ijbiomac.2018.03.028.

[14] Z. Wang et al., "Ultralight, highly compressible and fire-retardant graphene aerogel with self-adjustable electromagnetic wave absorption," Carbon, vol. 139, pp. 1126-1135, Nov. 2018, [Online]. Available: https://doi.org/10.1016/j.carbon.2018.08.014.

[15] W. S. Hummers and R. E. Offeman, "Preparation of graphitic oxide," J. Am. Chem. Soc., vol. 80, no. 6, pp. 1339-1339, Mar. 1958, [Online]. Available: https://doi.org/10.1021/ja01539a017.

[16] S. Wacławek, V. V. T. Padil, and M. Černík, "Major advances and challenges in heterogeneous catalysis for environmental applications: A review," Ecol. Chem. Eng. S, vol. 25, no. 1, pp. 9-34, Mar. 2018, [Online]. Available: https://doi.org/10.1515/eces-2018-0001.

[17] M. S. M. Wee, L. Matia-Merino, S. M. Carnachan, I. M. Sims, and K. K. T. Goh, "Structure of a shear-thickening polysaccharide extracted from the New Zealand black tree fern, Cyathea medullaris," Int. J. Biol. Macromol., vol. 70, pp. 86-91, Sep. 2014, [Online]. Available: https://doi.org/10.1016/j.ijbiomac.2014.06.032.

[18] M. Sims, A. M. Smith, G. A. Morris, M. U. Ghori, and S. M. Carnachan, "Structural and rheological studies of a polysaccharide mucilage from lacebark leaves (Hoheria populnea A. Cunn.)," Int. J. Biol. Macromol., vol. 111, pp. 839-847, May 2018, [Online]. Available: https://doi.org/10.1016/j.ijbiomac.2017.12.142.

[19] Shirwaikar, A. Shirwaikar, S. Prabhu, and G. Kumar, "Herbal excipients in novel drug delivery systems," Indian J. Pharm. Sci., vol. 70, no. 4, p. 415, 2008, [Online]. Available: https://doi.org/10.4103/0250-474X.44587.

[20] S. Patel and A. Goyal, "Applications of natural polymer gum arabic: A review," Int. J. Food Prop., vol. 18, no. 5, pp. 986-998, May 2015, [Online]. Available: https://doi.org/10.1080/10942912.2013.809541.

[21] C. Basavaraju, T. Demappa, and S. K. Rai, "Miscibility studies of polysaccharide xanthan gum and PEO (polyethylene oxide) in dilute solution," Carbohydr. Polym., vol. 69, no. 3, pp. 462-466, Jun. 2007, [Online]. Available: https://doi.org/10.1016/j.carbpol.2007.01.004.

[22] N. Jain, V. K. Singh, and S. Chauhan, "A review on mechanical and water absorption properties of polyvinyl alcohol based composites/films," J. Mech. Behav. Mater., vol. 26, pp. 213-222, 2017, [Online]. Available: https://doi.org/10.1515/jmbm-2017-0027.

[23] V. V. T. Padil, C. Senan, S. Wacławek, and M. Černík, "Electrospun fibers based on Arabic, karaya and kondagogu gums," Int. J. Biol. Macromol., vol. 91, pp. 299-309, 2016, [Online]. Available: https://doi.org/10.1016/j.ijbiomac.2016.05.064.

[24] N. V. Salim, X. Jin, and J. M. Razal, "Polyacrylonitrile/liquid crystalline graphene oxide composite fibers – Towards high performance carbon fiber precursors," Compos. Sci. Technol., vol. 182, p. 107781, 2019, [Online]. Available: https://doi.org/10.1016/j.compscitech.2019.107781.

[25] H. Kim, G. H. Shim, T. T. N. Vo, B. Kweon, K. M. Kim, and H. S. Ahn, "Building with graphene oxide: Effect of graphite nature and oxidation methods on the graphene assembly," RSC Adv., vol. 11, no. 6, pp. 3645-3654, 2021, [Online]. Available: https://doi.org/10.1039/D0RA10207E.

[26] N. G. de Barros et al., "Graphene oxide: A comparison of reduction methods," C (Basel), vol. 9, no. 3, p. 73, Jul. 2023, [Online]. Available: https://doi.org/10.3390/c9030073.

[27] H. Fujimoto, "Theoretical X-ray scattering intensity of carbons with turbostratic stacking and AB stacking structures," Carbon, vol. 41, no. 8, pp. 1585-1592, 2003, [Online]. Available: https://doi.org/10.1016/S0008-6223(03)00116-7.

[28] N. Popova, "Crystallographic analysis of graphite by X-ray diffraction," Coke Chem., vol. 60, no. 9, pp. 361-365, Sep. 2017, [Online]. Available: https://doi.org/10.3103/S1068364X17090058.

[29] Stobinski et al., "Graphene oxide and reduced graphene oxide studied by the XRD, TEM and electron spectroscopy methods," J. Electron Spectros. Relat. Phenomena, vol. 195, pp. 145-154, Aug. 2014, [Online]. Available: https://doi.org/10.1016/j.elspec.2014.07.003.

[30] H. A. Darwesh, S. B. Aziz, and S. A. Hussen, "Insights into optical band gap identification in polymer composite films based on PVA with enhanced optical properties: Structural and optical characteristics," Opt. Mater., vol. 133, p. 113007, Nov. 2022, [Online]. Available: https://doi.org/10.1016/j.optmat.2022.113007.

[31] S. S. Khasraw, D. M. Mamand, S. R. Saeed, et al., "Structural, morphological, and optical properties of PVA polymer composites incorporated with various concentrations of GO: Linear and nonlinear optoelectronic studies," J. Mater. Sci. Mater. Electron., vol. 36, p. 1067, 2025, [Online]. Available: https://doi.org/10.1007/s10854-025-15127-w.

[32] D. M. Mamand, D. M. Aziz, S. S. Khasraw, et al., "Improved optical characteristics of PEO polymer integrated with graphene oxide," Sci. Rep., vol. 15, p. 32225, 2025, [Online]. Available: https://doi.org/10.1038/s41598-025-16778-9.

[33] V. Salim, X. Jin, and J. M. Razal, "Polyacrylonitrile/liquid crystalline graphene oxide composite fibers – Towards high performance carbon fiber precursors," Compos. Sci. Technol., vol. 182, p. 107781, 2019, [Online]. Available: https://doi.org/10.1016/j.compscitech.2019.107781.

[34] R. M. Nezarati, M. B. Eifert, and E. Cosgriff-Hernandez, "Effects of humidity and solution viscosity on electrospun fiber morphology," Tissue Eng. Part C Methods, vol. 19, pp. 810-819, 2013, [Online]. Available: https://doi.org/10.1089/ten.tec.2012.0671.

[35] G. B. Medeiros, F. de A. Lima, D. S. de Almeida, et al., "Modification and functionalization of fibers formed by electrospinning: A review," Membranes (Basel), vol. 12, p. 861, 2022, [Online]. Available: https://doi.org/10.3390/membranes12090861.